

**CARBONACEOUS AND MAGNETITE-BEARING STARDUST COMETARY GRAINS FROM TRACKS 187, 188, 189, 190.** M. C. Price<sup>1</sup>, J. C. Bridges<sup>2</sup>, J. L. MacArthur<sup>2</sup> and L. J. Hicks<sup>2</sup>.<sup>1</sup>School of Physical Sciences, University of Kent, Canterbury, Kent, CT2 7NH, UK ([mcp2@star.kent.ac.uk](mailto:mcp2@star.kent.ac.uk)). <sup>2</sup>Space Research Centre, Dept. of Physics & Astronomy, University of Leicester, LE1 7RH, UK ([j.bridges@le.ac.uk](mailto:j.bridges@le.ac.uk)).

**Introduction:** We present Raman spectroscopy results from a set of terminal grains found in tracks C2112,4,187,0,0 ('187', 9 grains), C2045,2,188,0,0 ('188', 4 grains), C2045,3,189,0,0 ('189', 3 grains) and C2045,4,190,0,0 ('190', 3 grains) taken from the cometary side of NASA's *Stardust* mission sample collector [1]. In order to maximise the scientific return, it is vital that analyses of the samples are undertaken using as many different, non-destructive, techniques as possible - preferably on particles whilst they are still embedded in aerogel using, for example, Raman spectroscopy [2] and XRD [3].

**Methodology:** We used a *Labram-HR* Raman spectrometer at Kent to study the terminal grains. This spectrometer incorporates four lasers: 785 nm, 633 nm, 532 nm and 473 nm. The maximum laser power at was controlled by using a 10% neutral density filter which limited the power at the sample (through a  $\times 50$  objective) to a maximum of  $\sim 3$  mW, thus avoiding unwanted heating and possible modification of the grain [4]. Upon receipt, the keystones were carefully unwrapped and photographed. All tracks were mounted between thin (thickness unknown) silicon nitride windows, which greatly reduced fluorescence permitting all available excitation wavelengths to be used on these grains.

The samples have been analysed using Fe-K XAS and SR-XRD measurements at Beamline I18 of the *Diamond* synchrotron, UK. A spot size of  $2.5 \times 2.5 \mu\text{m}$  was used and Fe-K XAS was measured with the highest resolution over the Fe-K XANES region (7090–7125 eV), from which an absorption edge was estimated at 0.5 normalized intensity, and the  $1s \rightarrow 3d$  centroids were estimated as the intensity-weighted average of baseline-subtracted pre-edge peaks. The transmission SR-XRD measurements were taken between 9 – 15 keV, with a  $2\theta$  range of  $\sim 4.3^\circ$  to  $\sim 41.7^\circ$  corresponding to d-spacings of  $\sim 1 \text{ \AA}$  up to  $\sim 18 \text{ \AA}$ .

**Results:** Table 1 gives the ID ('TG' = Terminal Grain, 'SG' = subgrain) and the position of the subgrains relative to the largest terminal particle (denoted 'TG#1'). If viewed with the track entrance pointing south, then +ve X is west; +ve Y is south and +ve Z is into the aerogel. The detected composition of the grains are also given as well as contaminating aerogel (if detected).

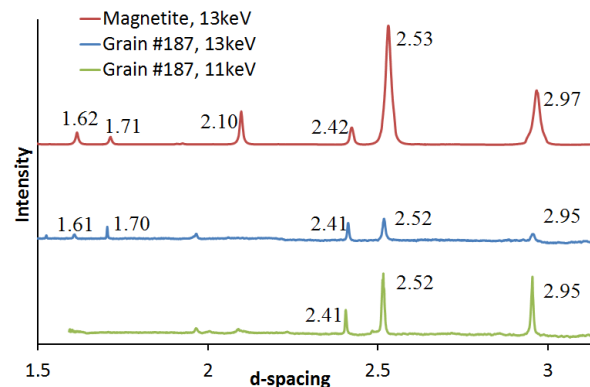


**Fig. 1.** SR-XRD identification of magnetite in the terminal grain of Track #187 through comparison of the  $2\theta$  peaks to a powdered magnetite standard.

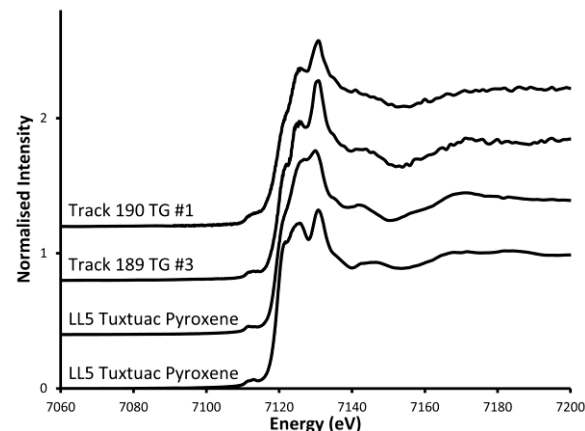


**Fig. 2.** Fe-K XANES plots of Track #189, #190 terminal grains compared to chondritic pyroxene. The #189 and #190 features around the absorption edges and white lines are characteristic of pyroxene.

**Track #187:** The main terminal grain has an iron-oxide type composition, with a (degraded) Raman spectrum indicative of magnetite mixed with some haematite. X-ray data confirms the presence of magnetite. (Fig. 1). The other terminal grain gave no detectable Raman signal with the 473 nm laser, but gave a very weak signature of carbon 'D' and 'G' bands when the 633 nm laser was used. Many subgrains are also present in the track, but gave no detectable Raman spectrum using either the 473 or 633 nm laser.

**Track #188:** The single terminal grain gave no detectable Raman signal under 473 or 633 nm laser wavelengths. One sub-grain gave an unidentified line at  $1200 \text{ cm}^{-1}$  and another had a weak carbon signal.

**Track #189:** The main terminal grain gave no Raman signal from the 473 nm laser, but a weak detection of ‘D’ and ‘G’ carbon lines was made with the 633 nm laser and confirmed with the 523 nm laser. No other Raman signals were detected from any of the other grains using 473, 532 or 633 nm wavelength lasers. However, Fe-K XANES (Fig. 2) is consistent with a pyroxene identity.

**Track #190:** Terminal grains gave no detectable signal under any laser wavelength. One sub-grain gave a weak carbon signal with the 633 nm wavelength laser. Fe-K XANES (Fig. 2) of the main terminal grain is consistent with a pyroxene identity.

It should be noted that tracks #189 and #190 are very closely spaced (separated by ~200 µm) and seem to have impacted the front surface of the aerogel at an angle of 10° from the normal.

### Conclusions:

- 1) A combination of SR-XRD, XANES and Raman reveals pyroxenes, magnetite and carbonaceous material in these terminal grains. There is increasing evidence that Wild-2 was magnetite rich, suggesting that the parent body underwent at least limited water-rock reactions [3]. Carbonaceous material seems to be concentrated around the bulb(s), possibly indicative of the (organic?) ‘glue’ that held the aggregate impactor together.
- 2) A range of different laser excitation wavelengths are needed to maximise the chances of identifying the composition of grains. More data need to be acquired using all four available laser wavelengths to maximise the chances of detecting the terminal and subgrain compositions.
- 3) Laser heating is a potential problem [5], and care has to be taken. A temperature calibration for olivine (and other minerals) is needed using Stokes/Anti-Stokes line ratios.

**References:** [1] Brownlee D. E. et al. (2006). *Science*, 314, 1711. [2] Wopenka B. (2012). *MAPS*, 47.4, 565. [3] Bridges et al. (2014). *45<sup>th</sup> LPSC, abstract #2015*. [4] Price M. C. et al. (2014). *45<sup>th</sup> LPSC abstract # 1252*. [5] Hibbert R. et al. (2014). *45<sup>th</sup> LPSC abstract #1350*.

**Table 1:** Raman analyses results from grains from tracks #187, #188, #189 and #190 (see text for description).

Grain ID	X, Y, Z (µm)	Composition	Grain ID	X, Y, Z (µm)	Composition
#187 TG #1	(0,0,0)	Possible magnetite/ haematite spectrum (mix?)	#188 TG #1	(0,0,0)	No detectable Raman signal
#187 TG #2	(+48.9,+64.5,-31.5)	Very weak carbon	#188 SG ‘a’	(-12.5,+355.9,+60.2)	Weak line at 1200 cm <sup>-1</sup>
#187 SG ‘a’	(+42.3, +131.6,-24.0)	No detectable Raman signal with 473 nm laser	#188 SG ‘b’	(-16.8,+408.5,+53.1)	Weak carbon bands
#187 SG ‘b’	(+22.0,+147.8, -32.4)	“	#188 SG ‘c’	(+6.6, +445.8, +56.8)	“
#187 SG ‘c’	(-6.0, +12.0, +9.1)	“	#189 TG #1	(0,0,0)	Very weak hint of Carbon with 532nm laser
#187 SG ‘d’	(-3.3, +30.2, +6.1)	“	#189 TG #2	(+38.1,+129.1,+71.4)	Weak hint of Carbon with 633nm laser
#187 SG ‘e’	(+4.1, +138.1, -13.0)	“	#189 TG #3	(-50.9, +172.1,+42.7)	No detectable signal with any laser
#187 SG ‘f’	(+26.8, +198.6,-10.4)	“	#190 TG #1	(0, 0, 0)	No detectable signal
#187 SG ‘g’	(+58.4, +97.0, -31.9)	“	#190 SG ‘a’	(+75.9, +42.5, +3.45)	Aerogel C-H lines
			#190 SG ‘b’	(+85.7, +617.2, +24.8)	Weak carbon